

Application of nanotitania and titania nanofibre in photocatalytic degradation of Rhodamine B in waste water

Suja N.R.* and Saumya Jos

Department of Chemistry, Maharaja's College, Ernakulam, Kochi -682 022, INDIA

*drsuja@maharas.ac.in

Abstract

Environmental protection is a key area in which a material like TiO_2 is playing a pivotal role. This study deals with the synthesis and characterisation of nano titania and titania fibre using a simple method. A comparative study of photo catalytic activity on the degradation of dye (Rhodamine B) in sunlight as well as using UV light was studied using TiO_2 nano particles, nanofibre and industrial titania. TiO_2 nano particle and nano-fibre were synthesized using Sol gel process and hydrothermal process respectively. Characterisation of the synthesised materials was done by IR, UV, SEM, XRD and TG studies.

Keywords: Nanotitania, titania fibre, photocatalytic activity, Rhodamine B, waste removal.

Introduction

As the world is becoming more and more aware of the need to preserve the environment, the quest to find materials that have a minimal impact on the eco-system is gaining momentum. One such material is titanium dioxide, which is known for its diverse advantages with less impact on the environment.

Titanium dioxide finds multiple applications as catalysts and catalyst supports, energy storage in solar cells¹⁶, photochemical degradation of toxic chemicals⁴ and as piezoelectric material²². The unique properties such as non-toxicity, chemical stability, corrosion resistance, good electrical properties, good congruence with various materials, high photo catalytic activity, high refractive index and ability to absorb ultraviolet (UV) light are important. Armed with these properties, TiO_2 nanoparticles are used in coatings^{3,17} in biological processes⁸ in catalytic properties like water splitting⁷ and in pollutant degradation¹, in body care products, in nano medicine, in lithium-ion batteries, in food packaging, in solar cells, in water purification and in gas sensors etc.

Nowadays, titanium dioxide is an indispensable photocatalytic substance that finds wide use. Titanium dioxide (TiO_2) is an n-type semiconductor with a ample direct band gap (3.2 eV). TiO_2 absorbs UV radiation (390 nm wavelength), but permits visible light to pass through very slowly. This is because of its extremely high refractive index in the visible area. Thermal stability includes nontoxicity, high free hydroxyl production, environmental

friendliness, biological and chemical inertness and cost-effectiveness. Use of titania for various application depends on the crystalline phases present, dimensions and morphology.

For multiple applications such as photocatalytic activity, designing of low dimensional nanostructures like nanofibres and nanotitania is important. Quite a few studies^{9,14,20} have been reported for the hydrothermal preparation of nanofibre. Industrial titania^{15,21} containing amorphous TiO_2 are octahedrally coordinated by both $-O-H$ groups and oxygen atoms, which are connected to titanium atoms of neighbouring octahedra. When compared to polymorphs of crystalline titania, it has a distinct structure. After being treated with sodium hydroxide, the caustic soda solution breaks part of the $Ti-O-H$ (and $Ti-O-Ti$) bonds to give rise to new coordinations.

The octahedra then interact with one another to provide long-range order, partially change into a layered titanate structure and self-assemble into tiny titanate nanosheets. Anisotropic proliferation of an increasing number of nanosheets could be the result of the hydrothermal reaction process and individual sheets could combine to produce nanofibers. Hydrothermal reaction could lead to the formation of more and more nanosheets with anisotropic multiplication and individual sheets may come together to give rise to nanofibers.

Using a facile method, this study explores the synthesis of titania nanomaterial and titania nanofiber and analyses and compares the crystalline phase, morphology and thermal stability. The photocatalytic activity was scrutinized in sunlight and UV light for the decomposition of Rhodamine B.

Material and Methods

Ethanol (Sigma Aldrich), Tween-20, Titanium (IV) isopropoxide (Sigma Aldrich), Industrial titania (20 nm), KOH (Sigma Aldrich), HCl (Sigma Aldrich), Rhodamine B dye and Deionized water were used.

Synthesis of TiO_2 nano particle: 20 mL of ethanol and 20 mL of deionized water were taken in a round bottom flask. To about 4% of the total mixture, 1.6 mL of stabilizer (Tween-20) was added. 0.2 mL of titanium (IV) isopropoxide were added and stirred for 3 hours at a reaction temperature of 50°C and then centrifuged at 10000 rpm for 10 minutes. It was washed with water and dried at room temperature.

Synthesis of TiO_2 nanofiber: About 156.25 mg of industrial titania (20 nm) was treated with 10 mL 10M KOH solution. The solution was transferred into a teflon-lined stainless-steel autoclave reactor and kept at 150°C for 21 hours. It was neutralized with 0.2 M HCl and centrifuged, washed five times with deionized water for 10 minutes at 10000 rpm and dried at room temperature. The samples were then calcined at 500°C.

Degradation of dye using TiO_2 nano particle: About 1.2 mg of Rhodamine B dye was made up to 500 mL in a standard flask. Take 100 mL of this solution in two beakers and added 1 and 5 mg of TiO_2 nano particle into it. It was sonicated for about 30 minutes. Keep under sunlight and record UV visible spectrum in intervals of 10 minutes. Repeat the same experiment in UV light.

Degradation of dye using TiO_2 nanofiber: The above procedure was repeated using TiO_2 nanofiber. Take UV visible spectrum in intervals of 10 minutes. A blank solution of dye was also kept under sunlight and degradation was analysed.

Scanning Electron Microscopy: Scanning electron microscopy was employed to analyse the surface morphology and structure characteristics of titania nanomaterial and fibre^{11,19}. All particles showed a uniform structure and no change in surface morphology of nano

titania was noticed. But titania fibre had a less crystalline nature as seen from SEM micrographs in figure 1.

TG and DTA analysis: The TG-DTA curves of dry TiO_2 nanoparticles¹⁸ are shown in the figures 2a and 2b. According to the TG analysis, there were two significant phases during the weight loss process of TiO_2 nanoparticle. One was that the weight loss rate was about 15% at temperatures ranging from room temperature to 300°C. It was mostly due to the desorption or release of various compounds in the powder such as adsorbed water. The next stage comprising of the loss of gel weight was not very noticeable at temperatures ranging from 300 to 700°C, which could be attributed to the desorption of the hydroxyl (OH) group on the nanoparticle TiO_2 . In titania according to Luca¹², surface OH groups are of two categories: terminal Ti-OH and nonterminal Ti-OH.

Dissociation temperatures of these surface OH groups differ from each other and there is a chance of each temperature being impacted by the chemical surroundings. Thus, the decrease in the weight appears in a wide range of temperatures. According to the DTA curve, a wide endothermic peak at 100 °C appeared, corresponding to the desorption of water. The TG¹³ of nanotitania showed an abrupt degradation of about 10% upto 100°C. The TG and DTA of titania nanofiber exhibit only a single weight loss and it was observed that nanofiber was more steady than nanotitania.

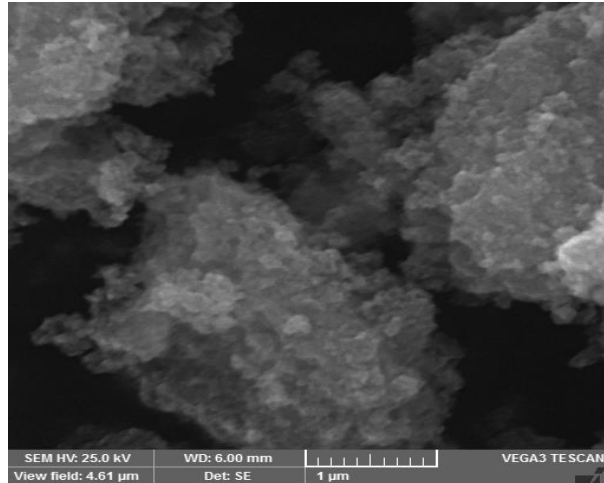
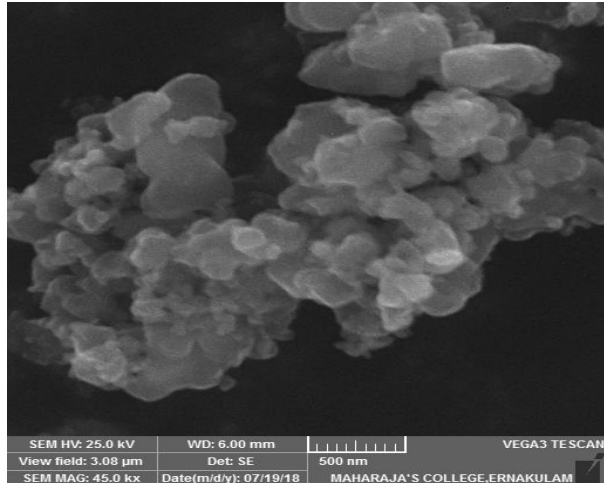


Figure 1: SEM micrographs of a) Nanotitania b) Nanofibre

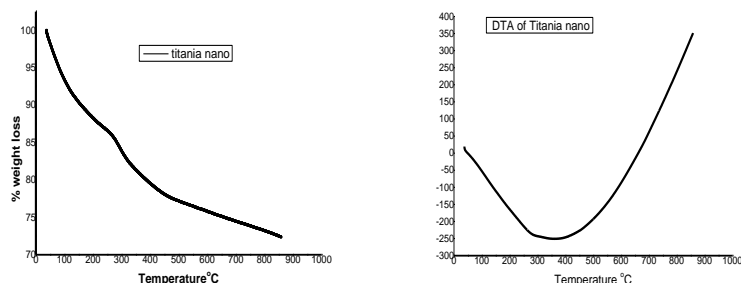


Figure 2: (a) TG of nanotitania (b) DTA of nanotitania

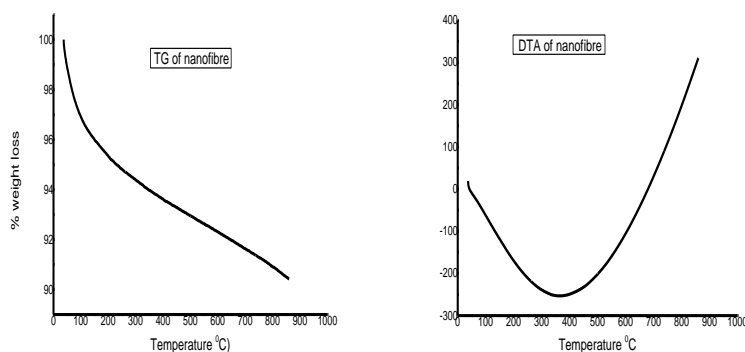


Figure 3: (a) TG of titania fiber (b) DTA of titania fiber

XRD data of titania nano and titania fiber: Figures 4 and 5 show the characteristic XRD patterns of the nanotitania and titania fibre. XRD was usually used for crystal phase identification and estimation of the anatase to rutile ratio as well as crystallite size of each phase present. The XRD² peaks at $2\theta = 25.25$ and 48 in the spectrum of nano TiO_2 were easily identified as the crystal of anatase form, whereas the XRD peaks at $2\theta = 27.42$ and 54.5 were easily identified as the crystal of rutile form. The XRD intensities of the anatase (101) peak and the rutile (110) peak were also analyzed. The percentage of anatase in the samples can be estimated from the respective integrated XRD peak intensities using the following equation:

$$X\% = 100/(1+1.265I_R/I_A)$$

where X is the wt% of anatase in the sample. The % of anatase to rutile phase in titania nanofibre is about 84:16 while the titania nano showed mainly the anatase phase only.

The crystallite size can also be determined from the broadening of corresponding X-ray spectral peaks by Scherrer formula:

$$L = k\lambda / (\beta \cos \theta)$$

where L is the crystallite size, λ is the wavelength of the X-ray radiation ($\text{Cu } \text{k}\alpha = 0.15418 \text{ nm}$), K is usually taken as 0.89 and β is the line width at half-maximum height. This is a generally accepted method to estimate the mean crystallite size of nanoparticle.

The particle size estimated by the above procedure in the case of nanotitania was about 10nm and that of nanofibre was 25nm. Figure 4 showed the XRD patterns of nanotitania. XRD peaks showed that only anatase phase exists in nanotitania as evident from the peak at $2\theta=25.25$ and 48 in figure 5 while both the phases exist in titania nanofiber.

As evident there are additional XRD peaks at $2\theta=27.42$ and 54.5 . This shows that phase transformation from amorphous to anatase and from anatase to rutile occurred in nanofiber.

The phase transformation from amorphous to anatase was completed at the temperature range from 450 to 550°C .

Diffuse reflectance spectra: The electronic transition for titania nano was spotted in the region 215, 256, 306, 396 nm and that for titania fibers was observed in the UV region from 224, 279, 348 and 391 nm. These peaks correspond to transitions from the top of the valence band to the bottom of the conduction band. This indicates that the bandgap energy of nanoparticle TiO_2 was 3.26 eV and that for the fibre was 3.17 eV respectively.

FTIR data of Titania fiber and Titania nanoparticle: FTIR spectra of titania fibre and titania nanoparticle demonstrated peaks at 3333, 1651 and 773 nm corresponding to $\text{Ti}-\text{O}-\text{Ti}$ stretching.

Photocatalytic activity in treatment of water containing dyes: Forgacs et al⁵ noted that conventional wastewater treatment technologies do not demonstrate effectiveness while handling wastewater of synthetic textile dyes because of the chemical stability of these pollutants. They went further to verify that 11 out of 18 azo dyes selected passed through the activated sludge process practically untreated. When it comes to chemical oxidants, most textile dyes are photocatalytically stable and refractory and these properties make them resistant towards decolorization by conventional biochemical and physico-chemical methods. All the aforementioned processes exhibit several deficiencies when it comes to removing dyes from wastewater.

Recently, studies were done on using photocatalysis⁶ in the removal of dyes from wastewater, particularly, because of its ability to completely mineralize the target pollutants. The present work is stated to review the effects of prepared titania fiber and titania nanomaterial on the photocatalytic degradation of textile dyes using like rhodamine B. TiO_2 , in its crystalline form, possesses much-coveted properties¹⁰ for application in homogenous and heterogeneous catalysis. As photocatalyst, titania has many advantages, especially when nanosized. They include photo-stability, thermal stability, reusability and durability, non-toxicity, low cost and water insolubility under most conditions.

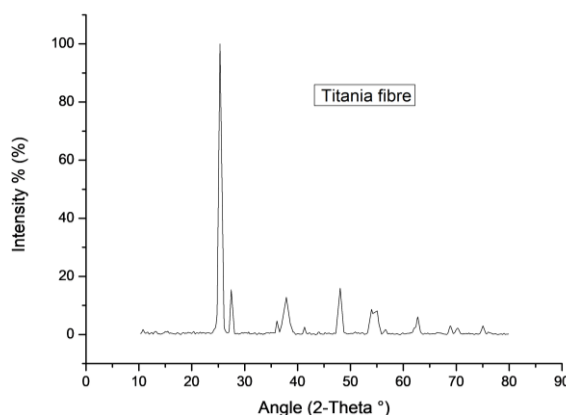


Figure 4: XRD pattern of titania fibre

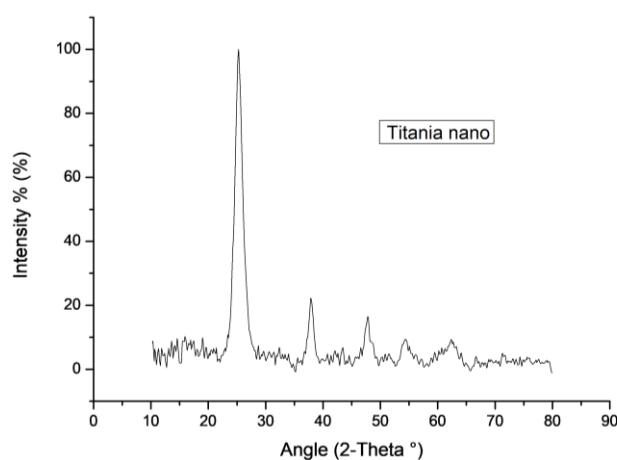


Figure 5: XRD of titania nano

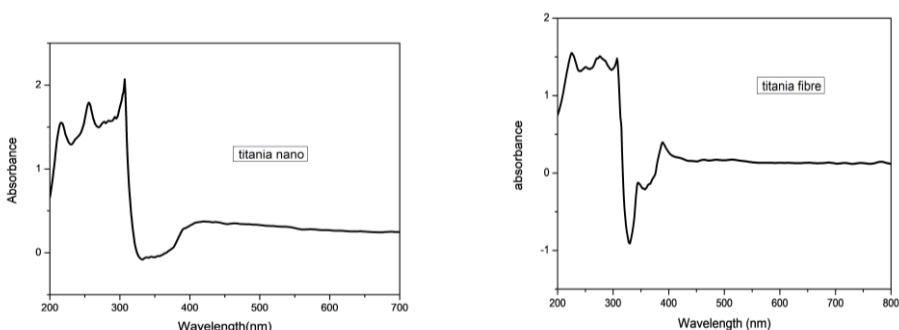


Figure 6: DRUV of a) titania nano b) titania fibre

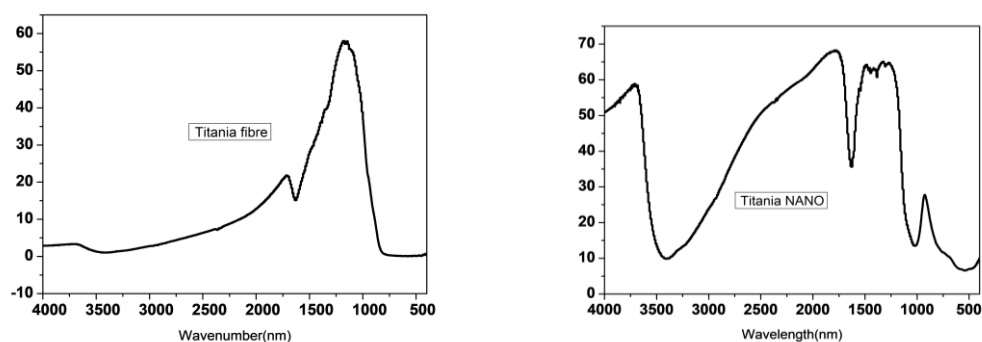


Figure 7: FTIR spectra of a) titania fibre b) titania nano

Unfortunately, pure TiO_2 does not absorb in the visible light region because of its high band gap energy of 3.2 eV (for bulk undoped TiO_2) which matches a wavelength of about 380 nm. One way to extend the light absorption of TiO_2 into the visible light region is to shift to absorption onset by modifying the surface properties of titania. This is done via doping, codeposition of metals, surface chelation and mixing of two semiconductors.

Results and Discussion

When it came to the degradation of rhodamine B in aqueous conditions, titania nanofiber and titania nanoparticles both showed activity. However, titania fibre exhibited more activity. This could be because of the presence of rutile phase in titania fibre. The statistics showed that both catalysts were active photocatalysts in both sunlight and UV light. The degradation rate spiked as the titania concentration was increased from 1 mg to 5 mg. The photocatalytic activity of the synthesised titania nanopowders was determined using Rhodamine B breakdown in aqueous solutions exposed to UV and visible light. Fluorescent lights (20 W Phillips lamps with UV intensity) placed at a distance of 20 cm from the top of the water solution were used to create UV light.

Photocatalysis reactions are initiated by the absorption of a photon with sufficient energy (equal to or greater than the catalyst's band-gap energy (E_b g)). Absorption brings about a charge separation by promoting an electron (e^-) from the valence band of the semiconductor catalyst to the conduction band, resulting in a hole (h^+) in the valence band. If a photocatalyst has to function efficiently, the electron-hole recombination should be avoided. Thus, the objective of the process is to have a reaction between the activated electrons and an oxidant to produce a reduced product and also a reaction between the generated holes and a reductant to produce an oxidized product.

The photogenerated electrons could reduce the dye or react with electron acceptors such as O_2 adsorbed on the $\text{Ti}(\text{III})$ -surface or dissolved in water, reducing it to superoxide radical anion $\text{O}_2\cdot^-$. Photogenerated holes can oxidise organic molecules to form R^+ or react with OH^- or H_2O to produce $\text{OH}\cdot$ radicals. They are thought to be responsible along with other highly oxidant species (peroxide radicals), for the heterogeneous TiO_2 photodecomposition of organic substrates as dyes. The resulting $\cdot\text{OH}$ radical is an extremely strong oxidising agent (typical redox potential +2.8 V) and may oxidise most azo dyes to mineral end products.

Table 1
Photocatalytic degradation using catalyst in UV and sunlight

Photocatalyst	Amount	Time	Sunlight % degradation	Ultraviolet light % degradation
Titania nano	1mg	30mts	56	32
Titania nano	1mg	1 hr	73	49
Titania fibre	5mg	30mts	61	-
Titania fibre	5mg	1hr	71	-
Titania fibre	1mg	30mts	37	35
Titania fibre	1mg	1 hr	54	53

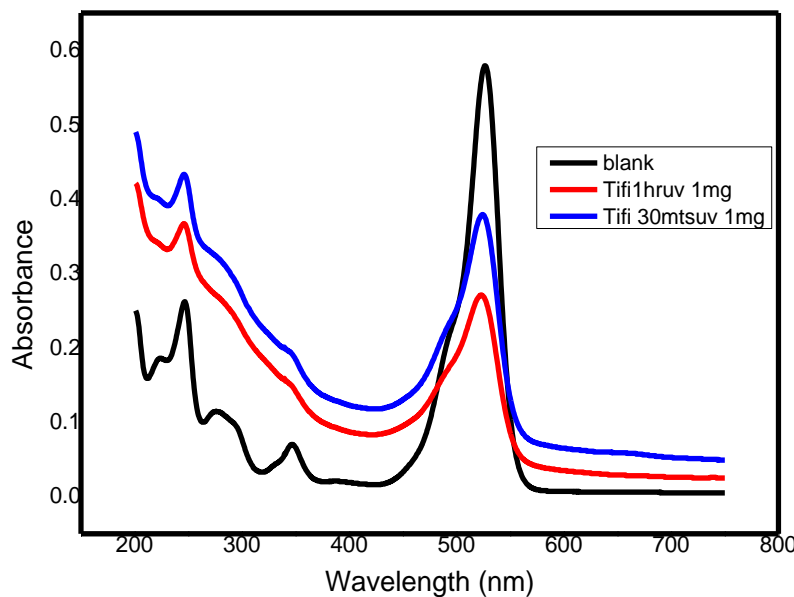


Figure 8: Degradation of Rh B Titania fibre UV light

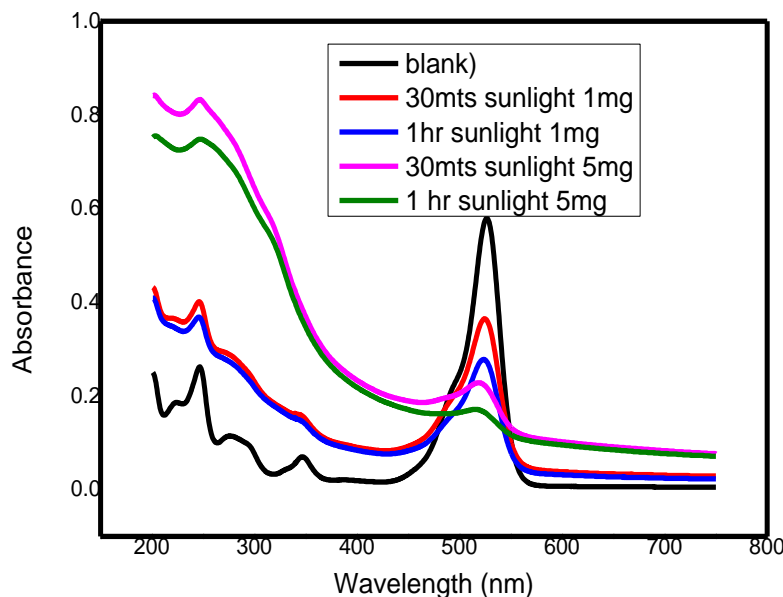


Figure 9: Effect of concentration of catalyst on Degradation of Rh B Titania fibre sunlight

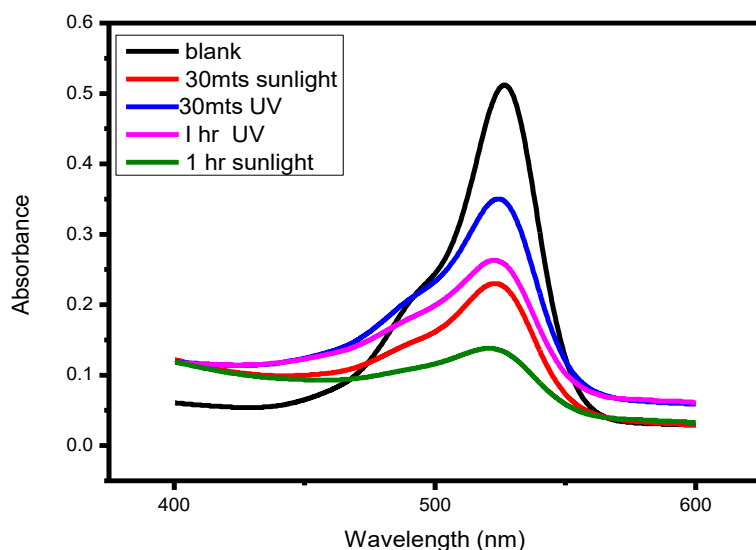


Figure 10: Degradation of Rh B using Titania nano sunlight and UV

Conclusion

The textile industry dumps large quantities of non-ecofriendly colours into water bodies. It is the need of the hour to develop methods to treat effluents and remove dangerous elements. This study was conducted to evaluate the role of Titania nano and Titania fibre in this process. The catalysts were synthesised and characterised by TG, XRD, SEM, FTIR and DRUV. Both catalysts demonstrated excellent photocatalytic activity in both sunlight and UV. The catalyst manifested good thermal stability. Titania fiber was more active in UV light through activity comparison and activity increased with catalyst concentration and time.

References

1. Akpan U.G. and Hameed B.H., Parameters affecting the photocatalytic degradation of dyes using TiO_2 -based photocatalysts: A review, *J. Hazard Mater.* **170**, 520 (2009)

2. Ba-Abbad M., Kadhum A.H., Mohamad A., Takriff M.S. and Sopian K., Synthesis and Catalytic Activity of TiO_2 Nanoparticles for Photochemical Oxidation of Concentrated Chlorophenols under Direct Solar Radiation, *Int. J. Electrochem. Sci.*, **7**, 4871 (2012)

3. Carneiro O., Teixeira V. and Portinha A., Iron-doped photocatalytic TiO_2 sputtered coatings on plastics for selfcleaning applications, *Mater. Sci. Eng. B*, **138**, 144 (2007)

4. Chen H., Nanayakkara C.E. and Grassian V.H., Titanium dioxide photocatalysis in atmospheric chemistry, *Chem. Rev.*, **112**, 5919 (2012)

5. Forgacs Esther, Cserháti Tibor and Orosb Gyula, Removal of synthetic dyes from wastewaters: A review, *Environ. Int.*, **30**, 953 (2004)

6. Fujishima Rao T.N. and Tryk D.A., Titanium dioxide photocatalysis, *J. Photochem. Photobiol. C: Photochem. Rev.*, **1**, 1 (2000)

7. Ismael Mohammed, Review and recent advances in solar-to-hydrogen energy conversion based on photocatalytic water splitting over doped-TiO₂ nanoparticles, *Solar Energy*, **211**, 522 (2020)

8. Jin C., Tang Y., Fan X.Y., Ye X.T., Li X.L., Tang K., Zhang Y.F., Li A.G. and Yang Y.J., *In vivo* evaluation of the interaction between titanium dioxide nanoparticle and rat liver DNA, *Toxicol. Ind. Health*, **29**(3), 235 (2013)

9. Kasuga T., Hiramatsu M., Hoson A., Sekino T. and Niihara K., Formation of titanium oxide nanotube, *Langmuir*, **14**, 3160 (1998)

10. Kiwi J., Role of oxygen at the TiO₂ interface during photodegradation of biologically difficult-to-degrade anthraquinone-sulfonate dyes, *Environ. Toxicol. Chem.*, **13**, 1569 (1994)

11. Li Y.F. and Liu Z.P., Particle size, shape and activity for photocatalysis on titania anatase nanoparticles in aqueous surroundings, *J. Am. Chem. Soc.*, **133**, 15743 (2011)

12. Luca Vittorio, Comparison of Size-Dependent Structural and Electronic Properties of Anatase and Rutile Nanoparticles, *J. Phys. Chem. C*, **113**, 6367 (2009)

13. Madarasz J., Okuya M., Varga P.P., Kaneko S. and Pokol G., TG/DTA-EGA-MS studies on titania precursors with low content of organics for porous thin films of TiO₂, *J. Anal. Appl. Pyrolysis*, **79**, 479 (2007)

14. Matsubara H., Takada M., Koyama S. and Hashimoto K., Fujishima A. Photoactive TiO₂ Containing Paper: Preparation and Its Photocatalytic Activity under Weak UV Light Illumination, *Chem. Lett.*, **24**(9), 767 (1995)

15. Norma A. Ramos-Delgado, Miguel Á. Gracia-Pinilla, Mangalaraja Viswanathan Ramalinga, O'Shea Kevin and Dionysiou D. Dionysios, Industrial synthesis and characterization of nanophotocatalysts materials: titania, *Nanotechnol Rev.*, **5**(5), 467 (2016)

16. O'Regan B. and Gratzel M., A low-cost, high-efficiency solar cell based on dyesensitized colloidal TiO₂ films, *Nature*, **353**, 737 (1991)

17. Othman Siti Hajar, Abdul Rashid Suraya, Idaty Mohd Ghazi Tinia and Abdullah Norhafizah, Dispersion and Stabilization of Photocatalytic TiO₂ Nanoparticles in Aqueous Suspension for Coatings Applications, *J. Nanomater.*, <https://doi.org/10.1155/2012/718214> (2012)

18. Ramya Chandrasekar et al, Fabrication and characterization of electrospun titania nanofibers, *J Mater Sci.*, **44**, 1198 (2009)

19. Soo-Jin Park, Yong C. Kang, Ju Y. Park, Ed A. Evans, Rex D. Ramsier and George G. Chase, Physical Characteristics of Titania Nanofibers Synthesized by Sol-Gel and Electrospinning Techniques, *Journal of Engineered Fibers and Fabrics*, **5**, 51 (2010)

20. Suzuki Yoshikazu, Pavasupree Sorapong and Yoshikawa Susumu, Natural rutile-derived titanate nanofibers prepared by direct hydrothermal processing, *J. Mater. Res.*, **20**, 1063 (2005)

21. Suzuki Y. and Yoshikawa S., Synthesis and thermal analyses of TiO₂-derived nanotubes prepared by the hydrothermal method, *J. Mater. Res.*, **19**, 982 (2004)

22. Yang Z., Liu X., Zhang C. and Liu B., A high-performance nonenzymatic piezoelectric sensor based on molecularly imprinted transparent TiO₂ film for detection of urea, *Biosens Bioelectron.*, **74**, 85 (2015).

(Received 17th May 2024, accepted 20th July 2024)